Modeling MIMO Fading Channels: Background, Comparison and Some Progress

Chengxiang Wang
Electrical, Electronic and Computer Engineering
Heriot-Watt University
Edinburgh EH14 4AS, UK
E-mail: cheng-xiang.wang@hw.ac.uk

Abstract— **The spatial correlation properties of multiple input multiple output (MIMO) channels can greatly affect the performance of MIMO systems. It is therefore important to develop MIMO channel models which can provide accurate spatial correlation characteristics. This paper starts with the brief review of MIMO channel models and then concentrates on investigating the spatial correlation characteristics of the Spatial Channel Model (SCM) in the Third Generation Partnership Project (3GPP) and the Kronecker Based Stochastic Model (KBSM) at three levels, namely the cluster level, link level, and system level. The KBSM has the spatial separability at all the three levels. The SCM shows the spatial separability at the link and system levels, but not at the cluster level since its spatial correlation is related to the joint distribution of the angle of arrival (AoA) and angle of departure (AoD). The KBSM with the Gaussian shaped Power Azimuth Spectrum (PAS) is found to fit best the 3GPP SCM in terms of the spatial correlations. Despite of its simplicity and analytical tractability, the KBSM is restricted to model only the average spatial behavior of MIMO channels. The SCM provides more insights of the variations of different MIMO channel realizations but the implementation complexity is relatively high.**

I. Introduction

In 3G and beyond-3G (B3G) wireless communication systems, higher data rate transmissions and better quality of services are demanded. By deploying spatially separated multiple antenna elements at both ends of the transmission link, MIMO technologies can improve the link reliability and provide a significant increase of the link capacity [1], [2]. However, the link capacity of MIMO systems is greatly affected by spatial correlation characteristics of the underlying MIMO channels [3]. An appropriate characterization and modeling of MIMO propagation channels is thus indispensable for the development of 3G and B3G systems.

In the literature, MIMO channels are often modeled by applying a stochastic approach [4][5]. Stochastic MIMO channel models can roughly be classified into three types [6], namely Geometrically Based Stochastic Models (GBSMs), Parametric Stochastic Models (PSMs), and Correlation Based Stochastic Models (CBSMs). It is important to mention that the above three types of stochastic MIMO channel models are interrelated. The relationship between a GBSM and a PSM was theoretically analyzed in [7], while the connection between a GBSM and a CBSM was demonstrated in [3]. There are only a few papers [8], [9] addressing the mapping between a PSM and a CBSM. Therefore, the spatial correlation properties of both types of models still require further investigation.

As a practical implementation of PSMs, the SCM was proposed by the 3GPP for both the link and system level simulations [10]. Since the spatial correlation properties of the SCM are implicit, it is difficult to directly connect its simulation results with theoretical multiuser MIMO analysis. On the other hand, KBSMs which are simplified CBSMs have received much attention. The reason is that KBSMs provide elegant and concise analytical expressions for MIMO channel spatial correlation matrices, making them easier to be integrated into a theoretical framework. However, compared with the SCM, KBSMs are often questioned about the over-simplification of MIMO channel characteristics. This paper is thus dedicated to fully investigate the spatial correlation properties of both the SCM and a KBSM. The interrelation and differences of the SCM and a KBSM will also be studied.

The rest of the paper is organized as follows. Section II briefly reviews the 3GPP SCM. Its spatial correlation characteristics are also analyzed. A KBSM and its spatial correlation properties are presented in Section III. Section IV compares the spatial correlation functions of both models from both the theoretical and simulation points of view. Finally, the conclusions are drawn in Section V.

II. The 3GPP SCM and Its Spatial Correlation Characteristics

The 3GPP SCM [10] emulates the double-directional and clustering effects for small scale fading mechanisms, and then adds shadowing, pathloss, and inter-site correlation effects for the purpose of system level simulations. Given an environment specified as either suburban macrocell, urban macrocell, or urban microcell, a set of user parameters is generated and is then used to generate the channel coefficients.

Let us now consider a downlink system where a base station (BS) transmits to a mobile station (MS). The received signal at the MS consists of N time-delayed paths of the transmitted signal. Each path further consists of M subpaths. Note that a path is resolvable and can be considered to correspond to a cluster of scatterers. Within a resolvable path (cluster), the subpaths are regarded as the unresolvable rays.

0-7803-9584-0/06/$20.00©2006 IEEE.

For an S element linear BS array and a U element linear MS array, the channel coefficients for one of N paths are given by a U-by-S matrix of complex amplitudes. By denoting the channel matrix for the nth path ($n = 1, \cdots, N$) as $\mathbf{H}_n(t)$, we can express the (u, s)th component ($s = 1, \cdots, S$ and $u = 1, \cdots, U$) of $\mathbf{H}_n(t)$ as follows [10]

$$\begin{aligned} h_{u,s,n}(t) &= \sqrt{\frac{P_n \sigma_{SF}}{M}} \sum_{m=1}^{M} \exp(j\Phi_{n,m}) \\ &\times \sqrt{G_{BS}(\theta_{n,m,AoD})} \exp[jkd_s \sin(\theta_{n,m,AoD})] \\ &\times \sqrt{G_{MS}(\theta_{n,m,AoA})} \exp[jkd_u \sin(\theta_{n,m,AoA})] \\ &\times \exp[jk \|\mathbf{v}\| \cos(\theta_{n,m,AoA} - \theta_v)t] \end{aligned} \quad (1)$$

where $j = \sqrt{-1}$; k is the wave number $2\pi/\lambda$ with λ denoting the carrier wavelength in meters; P_n is the power of the nth path; σ_{SF} is the lognormal shadow fading standard deviation; $G_{BS}(\theta_{n,m,AoD})$ and $G_{MS}(\theta_{n,m,AoA})$ are antenna gains of each array element at the BS and MS, respectively; d_s is the distance in meters from BS antenna element s to the reference ($s = 1$) antenna; d_u is the distance in meters from MS antenna element u to the reference ($u = 1$) antenna; $\Phi_{n,m}$ is the phase of the mth subpath of the nth tap; and $\|\mathbf{v}\|$ is the magnitude of the MS velocity vector. The angular parameters in (1) are shown in Fig. 1. Here, θ_v is the angle of the MS velocity vector with respect to the MS broadside, $\theta_{n,m,AoD}$ is the absolute AoD for the mth subpath of the nth tap at the BS with respect to the BS broadside, and $\theta_{n,m,AoA}$ is the absolute AoA for the mth subpath of the nth tap at the MS with respect to the BS broadside. From Fig. 1, the absolute AoD $\theta_{n,m,AoD}$ and AoA $\theta_{n,m,AoA}$ are given by [10]:

$$\begin{aligned} \theta_{n,m,AoD} &= \theta_{BS} + \delta_{n,AoD} + \Delta_{n,m,AoD} \\ &= \theta_{n,AoD} + \Delta_{n,m,AoD} \end{aligned} \quad (2)$$

$$\begin{aligned} \theta_{n,m,AoA} &= \theta_{MS} + \delta_{n,AoA} + \Delta_{n,m,AoA} \\ &= \theta_{n,AoA} + \Delta_{n,m,AoA} \end{aligned} \quad (3)$$

respectively, where θ_{BS} is the line-of-sight (LOS) AoD direction between the BS and MS with respect to the broadside of the BS array, θ_{MS} is the angle between the BS-MS LOS and the MS broadside, $\delta_{n,AoD}$ is the AoD for the nth path with respect to the LOS AoD, $\delta_{n,AoA}$ is the AoA for the nth path with respect to the LOS AoA, $\Delta_{n,m,AoD}$ and $\Delta_{n,m,AoA}$ are the offsets for the mth subpath of the nth path with respect to $\delta_{n,AoD}$ and $\delta_{n,AoA}$, respectively. Note that $\theta_{n,AoD} = \theta_{BS} + \delta_{n,AoD}$ and $\theta_{n,AoA} = \theta_{MS} + \delta_{n,AoA}$ are called the mean AoD and mean AoA, respectively.

According to the construction of the absolute subpath AoD in (2) and the absolute subpath AoA in (3), we can distinguish the SCM properties at three levels, namely the cluster level, link level, and system level. At the cluster level, the mean AoD $\theta_{n,AoD}$ and mean AoA $\theta_{n,AoA}$ are kept constant. The subpath statistics are emulated by the specified constant values of subpath AoD offsets $\Delta_{n,m,AoD}$ and subpath AoA offsets $\Delta_{n,m,AoA}$. This means that for all the cluster level simulations,

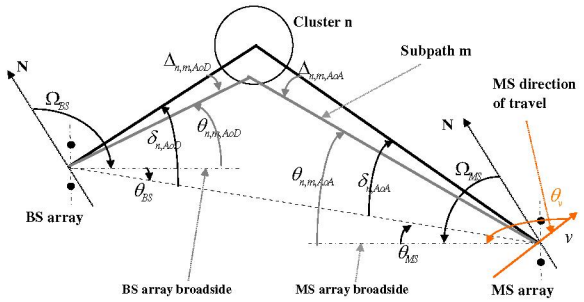

Fig. 1. BS and MS angle parameters in the 3GPP SCM [10].

the cluster position is fixed while a given scatterer distribution is used. At the link level, θ_{BS} and θ_{MS} are still kept constant, while $\delta_{n,AoD}$ and $\delta_{n,AoA}$ are random variables [10]. It follows that the link level properties of the SCM are obtained by taking the average of the corresponding functions of the SCM at the cluster level over all the realizations of $\delta_{n,AoD}$ and $\delta_{n,AoA}$. Clearly, link level characteristics are related to cluster distributions. At the system level, θ_{BS}, θ_{MS}, $\delta_{n,AoD}$, and $\delta_{n,AoD}$ are all random variables. It is important to mention that the actual values of θ_{BS} and θ_{MS} depend on the placement of the MS with respect to each BS, which is determined according to the cell layout and the broadside of the instant antenna array orientations. If both θ_{BS} and θ_{MS} are random variables, we actually consider multiple BSs and MSs. Without loss of generality, in this paper both of them are treated as independent random variables uniformly distributed from 0 to 2π. Similarly, the system level properties are obtained by averaging all realizations of θ_{BS} and θ_{MS} based on the relative BS-MS position statistics.

Since the focus of our studies is on the spatial correlation properties of the SCM related to only the small scale fading, we can simplify (1) by neglecting irrelevant components: the pathloss and shadowing factors. Moreover, we assume that omnidirectional antenna elements are employed in both the BS and MS arrays, i.e., $G_{BS}(\theta_{n,m,AoD}) = G_{MS}(\theta_{n,m,AoA}) = 1$. It follows that (1) is reduced to

$$\begin{aligned} h_{u,s,n}(t) &= \sqrt{\frac{P_n}{M}} \sum_{m=1}^{M} \exp[jkd_s \sin(\theta_{n,m,AoD})] \\ &\times \exp[jkd_u \sin(\theta_{n,m,AoA})] \exp(j\Phi_{n,m}) \\ &\times \exp[jk \|\mathbf{v}\| \cos(\theta_{n,m,AoA} - \theta_v)t]. \end{aligned} \quad (4)$$

The complex spatial correlation function between two arbitrary channel coefficients connecting two different sets of antenna elements is defined as

$$\rho_{s_2 u_2}^{s_1 u_1} = E\left\{ \frac{h_{u_1,s_1,n}(t) h_{u_2,s_2,n}^*(t)}{\sigma_{h_{u_1,s_1,n}} \sigma_{h_{u_2,s_2,n}}} \right\} \quad (5)$$

where $\sigma_{h_{u_1,s_1,n}} = \sqrt{P_n}$ and $\sigma_{h_{u_2,s_2,n}} = \sqrt{P_n}$ are the standard deviations of $h_{u_1,s_1,n}$ and $h_{u_2,s_2,n}$, respectively. The

substitution of (4) into (5) results in

$$\rho_{s_2u_2}^{s_1u_1} = \frac{1}{M}\sum_{m=1}^{M} E\{\exp[jk\Delta d_s \sin(\theta_{n,m,AoD})] \times \exp[jk\Delta d_u \sin(\theta_{n,m,AoA})]\} \quad (6)$$

where $\Delta d_s = |d_{s_1} - d_{s_2}|$ denotes the relative BS antenna element spacing and $\Delta d_u = |d_{u_1} - d_{u_2}|$ denotes the relative MS antenna element spacing. Note that $E\{\exp(\Phi_{n,m_1} - \Phi_{n,m_2})\} = 0$ when $m_1 \neq m_2$ has been used in the derivation of (6). Some special cases of (6) can be observed:

(i) $\Delta d_s = 0$: Two links share the same transmit antenna element. The spatial correlation function at the MS is

$$\rho_{u_1u_2}^{MS} = \frac{1}{M}\sum_{m=1}^{M} E\{\exp[jk\Delta d_u \sin(\theta_{n,m,AoA})]\}. \quad (7)$$

(ii) $\Delta d_u = 0$: Two link share the same receive antenna element. The spatial correlation function at the BS is

$$\rho_{s_1s_2}^{BS} = \frac{1}{M}\sum_{m=1}^{M} E\{\exp[jk\Delta d_s \sin(\theta_{n,m,AoA})]\}. \quad (8)$$

It is obvious that the spatial correlation function (6) cannot be broken down into the multiplication of a receive term (7) and a transmit term (8). This indicates that the spatial correlation function of the 3GPP SCM is not separable. Consequently, the spatial correlation matrix $\mathbf{R}_{\mathrm{MIMO}}$ of the SCM cannot be written as the Kronecker product of $\mathbf{R}_{\mathrm{BS}}$ and $\mathbf{R}_{\mathrm{MS}}$. Here, $\mathbf{R}_{\mathrm{BS}}$ and $\mathbf{R}_{\mathrm{MS}}$ denote the spatial correlation matrices at the BS and MS, respectively.

(iii) $M \to \infty$: We can rewrite (6) as

$$\lim_{M\to\infty} \rho_{s_2u_2}^{s_1u_1} = \int_0^{2\pi}\int_0^{2\pi} \{\exp[jk\Delta d_s \sin(\phi_{n,AoD})] \times \exp[jk\Delta d_u \sin(\phi_{n,AoA})] \times p_{us}(\phi_{n,AoD}, \phi_{n,AoA}) d\phi_{n,AoD} d\phi_{n,AoA} \quad (9)$$

where $p_{us}(\phi_{n,AoD}, \phi_{n,AoA})$ represents the joint probability density function (PDF) of the AoD and AoA.

(iv) $\Delta d_s = 0$ and $M \to \infty$: We can rewrite (7) as

$$\lim_{M\to\infty} \rho_{u_1u_2}^{MS} = \int_0^{2\pi} \exp[jk\Delta d_u \sin(\phi_{n,AoA})] \times p_u(\phi_{n,AoA}) d\phi_{n,AoA} \quad (10)$$

where $p_u(\phi_{n,AoA})$ stands for the PDF of the AoA.

(v) $\Delta d_u = 0$ and $M \to \infty$: We can rewrite (8) as

$$\lim_{M\to\infty} \rho_{s_1s_2}^{BS} = \int_0^{2\pi} \exp[jk\Delta d_s \sin(\phi_{n,AoD})] \times p_s(\phi_{n,AoD}) d\phi_{n,AoD} \quad (11)$$

where $p_s(\phi_{n,AoD})$ denotes the PDF of the AoD. Similarly, we cannot write (9) simply as the product of (10) and (11). Therefore, the Kronecker structure is not fulfilled for the spatial correlation of the 3GPP SCM.

III. The KBSM and Its Spatial Correlation Characteristics

The KBSM assumes that the channel coefficients of a narrowband MIMO channel are complex Gaussian distributed with identical average power [4]. The channel can therefore be fully characterized by its first and second order statistics.

As for the SCM, let us still consider a downlink transmission system with an S element linear BS array and a U element linear MS array. The complex spatial correlation function at the BS between antenna elements s_1 and s_2 is given by [11]

$$\hat{\rho}_{s_1s_2}^{BS} = \int_0^{2\pi} \exp[jk\Delta d_s \sin(\hat{\theta}_{AoD})] \hat{p}_s(\hat{\theta}_{AoD}) d\hat{\theta}_{AoD}. \quad (12)$$

In (12), $\hat{p}_s(\hat{\theta}_{AoD})$ denotes the PAS related to the AoD. In the literature, different functions have been proposed for the PAS, such as a cosine raised function [12], a Gaussian function [13], a uniform function [14], and a Laplacian function [15]. Note that the PAS here has been normalized in such a way that $\int_0^{2\pi} \hat{p}_s(\hat{\theta}_{AoD}) d\hat{\theta}_{AoD} = 1$ is fulfilled. Therefore, $\hat{p}_s(\hat{\theta}_{AoD})$ is actually identical with the PDF of the AoD $\hat{\theta}_{AoD}$. Analogous to the AoD for the SCM in (2), $\hat{\theta}_{AoD}$ can also be written as $\hat{\theta}_{AoD} = \hat{\theta}_{0,AoD} + \Delta\hat{\theta}_{AoD}$, where $\hat{\theta}_{0,AoD}$ and $\Delta\hat{\theta}_{AoD}$ denote the mean AoD and the subpath AoD offset, respectively.

Similarly, the spatial correlation functions at the MS between antenna elements u_1 and u_2 can be expressed as

$$\hat{\rho}_{u_1u_2}^{MS} = \int_0^{2\pi} \exp[jk\Delta d_u \sin(\hat{\theta}_{AoA})] \hat{p}_u(\hat{\theta}_{AoA}) d\hat{\theta}_{AoA} \quad (13)$$

where $\hat{p}_u(\hat{\theta}_{AoA})$ is the PAS related to the AoA. Due to the normalization, $\hat{p}_u(\hat{\theta}_{AoA})$ is also regarded as the PDF of the AoA. Analogously, we have $\hat{\theta}_{AoA} = \hat{\theta}_{0,AoA} + \Delta\hat{\theta}_{AoA}$.

The KBSM further assumes that $\hat{\rho}_{s_1s_2}^{BS}$ and $\hat{\rho}_{u_1u_2}^{MS}$ are independent of u and s, respectively. This implies that the AoD and AoA are independently distributed and the spatial correlation function $\hat{\rho}_{s_2u_2}^{s_1u_1}$ between two arbitrary channel coefficients is simply the product of $\hat{\rho}_{s_1s_2}^{BS}$ and $\hat{\rho}_{u_1u_2}^{MS}$, i.e.,

$$\hat{\rho}_{s_2u_2}^{s_1u_1} = \hat{\rho}_{s_1s_2}^{BS}\hat{\rho}_{u_1u_2}^{MS} = \int_0^{2\pi} \exp[jk\Delta d_u \sin(\hat{\theta}_{AoA})] \hat{p}_s(\hat{\theta}_{AoA}) d\hat{\theta}_{AoA} \times \int_0^{2\pi} \exp[jk\Delta d_s \sin(\hat{\theta}_{AoD})] \hat{p}_u(\hat{\theta}_{AoD}) d\hat{\theta}_{AoD}. \quad (14)$$

In matrix form, the spatial correlation matrix $\hat{\mathbf{R}}_{\mathrm{MIMO}}$ of the MIMO channel can be described as the Kronecker product of the spatial correlation matrix $\hat{\mathbf{R}}_{\mathrm{BS}}$ at the BS and $\hat{\mathbf{R}}_{\mathrm{MS}}$ at the MS, i.e., [4]

$$\hat{\mathbf{R}}_{\mathrm{MIMO}} = \hat{\mathbf{R}}_{\mathrm{BS}} \otimes \hat{\mathbf{R}}_{\mathrm{MS}} \quad (15)$$

where $\otimes$ represents the Kronecker product. For example, a 2×2 MIMO channel with the transmitter correlation function $\hat{\rho}_t = \hat{\rho}_{s_1s_2}^{BS}$ and the receiver correlation function $\hat{\rho}_r = \hat{\rho}_{u_1u_2}^{MS}$

gives the channel correlation matrix as:

$$\hat{\mathbf{R}}_{\text{MIMO}} = \begin{bmatrix} 1 & \hat{\rho}_r & \hat{\rho}_t & \hat{\rho}_r\hat{\rho}_t \\ \hat{\rho}_r^* & 1 & \hat{\rho}_r\hat{\rho}_t^* & \hat{\rho}_t \\ \hat{\rho}_t^* & \hat{\rho}_r^*\hat{\rho}_t & 1 & \hat{\rho}_r \\ \hat{\rho}_r^*\hat{\rho}_t^* & \hat{\rho}_t^* & \hat{\rho}_r^* & 1 \end{bmatrix}. \quad (16)$$

IV. Spatial Correlation Comparison Between the SCM and KBSM

In this section, we compare the spatial correlation characteristics of the SCM and the KBSM from both the theoretical and simulation points of view.

The comparison of (6) and (9) clearly shows the fundamental difference between the SCM and KBSM. The SCM assumes a finite number of subpaths in each path, whereas a KBSM simply assumes a very large or even infinite number of multipath components. The AoD and the AoA are assumed to be independently distributed in the KBSM, while correlated in the SCM. This is also the reason why the spatial correlation function is separable for the KBSM but not for the SCM. On the other hand, both models tend to have equivalent spatial correlation properties under all of the following three conditions: 1) The number M of subpaths in each path for the SCM tends to infinity. 2) Two links share the same antenna element at one end, i.e., $\Delta d_s = 0$ or $\Delta d_u = 0$. This corresponds to the spatial correlation functions at either the MS or the BS. 3) The same set of angle parameters including the same PAS are used for both models. The above conditions are obvious by comparing (10) and (13), (11) and (12).

For the SCM, fixed values are chosen for the subpath AoA and AoD offsets. For the KBSM, however, the subpath PAS functions can have different candidates [12]-[15]. Our first task is to find out which functions should be employed for the PDFs of subpath AoD and AoA offsets in the KBSM in order to fit well its spatial correlation properties to those of the SCM with the given set of parameters.

From the above discussions, the best fit subpath PASs for the KBSM should give the smallest difference with the interpolated SCM in terms of the spatial correlation functions at the BS and MS. Therefore, for the SCM, we interpolated subpath angle offsets 100 times to approach the assumption of $M \to \infty$, and then calculate the envelope correlations at the BS/MS as functions of the antenna spacing and mean AoD/AoA according to (10) and (11), using the method of numerical integral. Similarly, for the KBSM, we calculated the BS/MS envelope correlation functions with different PAS functions (uniform, Gaussian, Laplacian) by using the method of Bessel series expansion [11]. We found that in all the three cases (AS= 2, 5, and 35 degrees), the KBSM with the Gaussian shape PAS provides the best fitting to the interpolated SCM. We note that even for the original SCM model with $M = 20$ and correlations functions given as (7) and (8), the Gaussian shape PASs also provide the best fittings. Fig. 2 shows an interception of this fitting process by imposing the normalized antenna spacings equal to 2 and draws the spatial correlation functions against the mean AoA/AoD. Fig. 3 shows another interception by setting the mean AoA/AoD

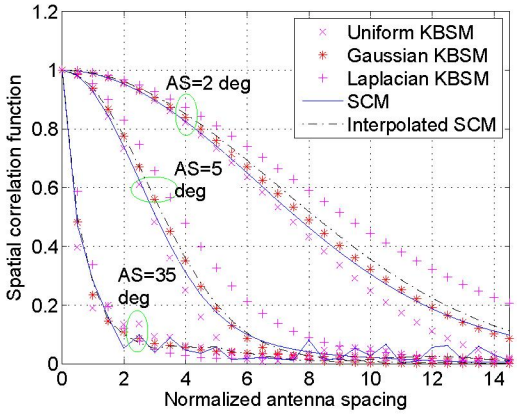

Fig. 2. Spatial correlation functions of the SCM, interpolated SCM, and KBSMs with uniform, Gaussian, and Laplacian PASs (mean AoA/AoD = 60 degree)

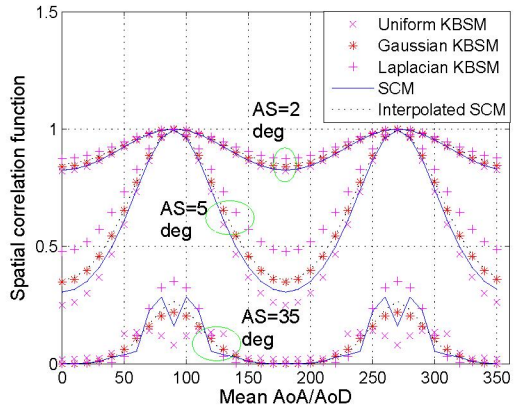

Fig. 3. Spatial correlation functions of the SCM, interpolated SCM, and KBSMs with uniform, Gaussian, and Laplacian PASs (normalized antenna spacing = 2).

to 60 degree and plots the spatial correlations as functions of the normalized antenna spacing. In both figures, it is obvious that the KBSM with the Gaussian PASs provide the best fitting to both the SCM and interpolated SCM. This result is interesting considering the fact that 3GPP actually suggested a Laplacian distribution for the AoD PAS and either a Laplacian or a uniform distribution for the AoA PAS in its link level calibration [10]. Moreover, in both figures, the spatial correlation functions obtained from the SCM are observed to have unstable fluctuations around the ideal values approximated by the interpolated SCM. This is caused by the so-called "implementation lost" due to the insufficient number M of subpaths used in the SCM. It is therefore suggested that the employed number of subpaths in the 3GPP SCM should be increased in order to improve its simulation accuracy. In the following, we will compare the spatial correlation properties of the SCM and the KBSM with Gaussian PASs at three levels.

Fig. 4 visualizes the theoretical cluster level envelope corre-

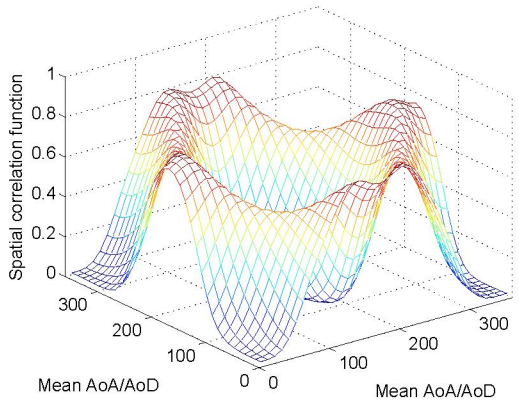

Fig. 4. The cluster level spatial correlation function of the SCM as a function of the mean AoA and mean AoD ($\Delta d_s/\lambda = 2$, $\Delta d_u/\lambda = 0.5$, BS AS = 5 degree, MS AS = 35 degree).

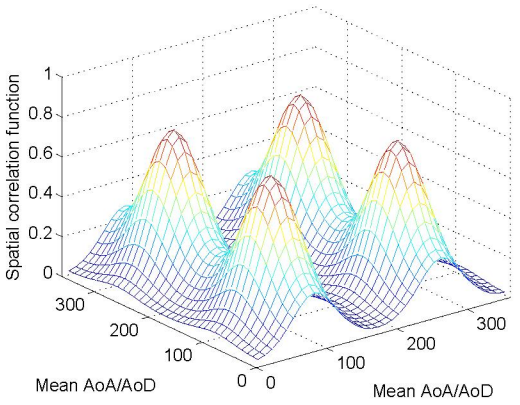

Fig. 5. The cluster level spatial correlation function of the KBSM as a function of the mean AoA and mean AoD ($\Delta d_s/\lambda = 2$, $\Delta d_u/\lambda = 0.5$, Gaussian PDFs for both the subpath AoD and AoA offsets).

lation function of the SCM against both the mean AoA $\theta_{n,AoA}$ and mean AoD $\theta_{n,AoD}$. The normalized antenna spacings are set to be 2 at the BS ($\Delta d_s/\lambda = 2$) and 0.5 at the MS ($\Delta d_u/\lambda = 0.5$). The subpath AoD offsets $\Delta_{n,m,AoD}$ and the subpath AoA offsets $\Delta_{n,m,AoA}$ are taken from (Table 5.2 in [10]), where the ASs for the BS and MS are set to be 5 degree and 35 degree, respectively. This corresponds to an urban microcell scenario in the SCM. Note that Fig. 4 is plotted based on (6) without taking the average, i.e., $E\{\cdot\}$ is omitted since all the relevant parameters are not random variables. In Fig. 5, the theoretical cluster level envelope correlation function $\left|\hat{\rho}_{s_2u_2}^{s_1u_1}\right|^2$ of the KBSM (see (14)) is shown against both the mean AoA $\hat{\theta}_{0,AoA}$ and mean AoD $\hat{\theta}_{0,AoD}$. Again, $\Delta d_s/\lambda = 2$ and $\Delta d_u/\lambda = 0.5$ are used. The PDFs of the subpath AoD offsets $\Delta\hat{\theta}_{AoD}$ and the subpath AoA offsets $\Delta\hat{\theta}_{AoA}$ follow the corresponding Gaussian functions, as concluded from the above discussions. A significant difference between Figs. 4 and 5 is observed, which indicates that the SCM and the KBSM do not agree well in terms of the instant spatial correlation at the cluster level when the two links under consideration come from different antenna pairs.

At the link level, the cluster position parameters $\delta_{n,AoD}$ and $\delta_{n,AoA}$ are treated as random variables. At the system level, in addition, the link position parameters θ_{BS} and θ_{MS} are treated as random variables. It is difficult to provide closed form expressions for the link and system level correlation characteristics. Therefore, we will evaluate them by simulations.

Without loss of generality, a 2×2 MIMO link is considered for simulations. Two models are put into the same framework by integrating the KBSM into the 3GPP SCM and share the SCM parameter generator [16]. It is important to mention that our comparison method differs from the methods in [8] and [17], where not the same set of parameters is used for both the SCM and KBSM. The simulation procedure is as follows. Channel coefficients are generated for the SCM based on each realization of the parameter set Ψ. The spatial correlation functions for an arbitrary path are then evaluated numerically, resulting in a 4×4 channel correlation matrix $\mathbf{R}_{\text{MIMO}}$. For the KBSM, the angular parameters from Ψ are again used to calculate $\hat{\mathbf{R}}_{\text{MIMO}}$ based on (12)–(16). We then focus on comparing the first column of $\mathbf{R}_{\text{MIMO}}$ and $\hat{\mathbf{R}}_{\text{MIMO}}$, i.e, the correlation function at the BS (s_1u_1,s_2u_1), the correlation function at the MS (s_1u_1,s_1u_2), and the cross-channel correlation function (s_1u_1,s_2u_2). In addition, the results shown in Figs. 6 and 7 are based on the real-valued envelope correlation function ρ_e given by $\rho_e = |\rho_c|^2$, where ρ_c denotes the complex correlation function.

Taking the statistical average of the spatial correlation functions at the cluster level over 400 realizations of the cluster position parameters $\delta_{n,AoD}$ and $\delta_{n,AoA}$ leads to our link level simulation results. Imposing $\theta_{BS} = 60$ degree, $\theta_{MS} = 245$ degree, and $\Delta d_u = 0.2\lambda$, Fig. 6 shows the spatial correlation functions of both the SCM and KBSM, against the normalized BS antenna spacing $\Delta d_s/\lambda$. Very good agreements are observed in all cases. Thus we can conclude that at the link level, 1) effects of the "implementation loss" and the imperfect PAS fitting tend to be averaged out; 2) the SCM has the same property of the spatial separability as the KBSM when taking the average at the link level.

Similar to link level simulations, Fig. 7 shows the results of system level simulations at the BS of both models by imposing $\Delta d_s = 0.2\lambda$ and $\Delta d_u = 0.2\lambda$, respectively. Again, good agreements are observed in all cases. Therefore, a conclusion can be drawn that the spatial separability of the KBSM is also the property of the SCM at the system level. Note that the spatial correlation function at the BS (s_1u_1,s_2u_1) in Fig. 7 approximates the well-known Bessel function given as $\left|J_0(2\pi\frac{\Delta d_s}{\lambda})\right|^2$. This is because of the fact that at the system level, θ_{BS} are considered as random variables uniformly distributed over $[0, 2\pi)$.

V. Conclusion

In this paper, we have extensively investigated and compared the spatial correlation characteristics of the 3GPP SCM and KBSM. Theoretical studies clearly show that the spatial correlation of the SCM is related to the joint distribution of the AoA and AoD, while the KBSM calculates the spatial correlation from independent AoA and AoD distributions. Under the conditions that the number of subpaths tends to infinity in the SCM, two correlated links share one antenna at either end, and the same set of angle parameters are used, the two models tend to be equivalent. Compared with uniform and Laplacian functions, it turns out the Gaussian shaped PAS enables the KBSM to best fit the 3GPP SCM in terms of the spatial correlation functions. Simulation results demonstrate that the spatial separability is observed for the SCM only at the link and system levels, not at the cluster level. The KBSM, however, exhibits the spatial separability at all the three levels.

Although the KBSM has the advantages of simplicity and analytical tractability, it only describes the average spatial properties of MIMO channels. On the other hand, the SCM is more complex but allows us to sufficiently simulate the variations of different MIMO channel realizations.

References

[1] I. E. Talatar, "Capacity of Muli-antenna Gaussian Channels," *Tech. Rep., AT&T Bell Labs*, June 1995.

[2] G. J. Foschini and M. J. Gans, "On limits of wireless communications in a fading environment," *Wireless Personal Communications*, issue 6, pp. 311–335, 1998.

[3] D. S. Shiu, G. J. Foschini, M. J. Gans and J. M. Kahn, "Fading correlation and its effect on the capacity of multielement antenna systems," *IEEE Trans Commun.*, vol. 48, no. 3, pp. 502–513, Mar. 2000.

[4] J. P. Kermoal, L. Schumacher, K. I. Pedersen and P. E. Mogensen, "A stochastic MIMO radio channel model with experimental validation," *IEEE J. on Selective Areas in Commun.*, vol. 20, no. 6, pp. 1211–1226, Aug. 2002.

[5] A. Abdi, J. A. Barger and M. Kaveh, "A parametric model for the distribution of the angle of arrival and the associated correlation function and power spectrum at the mobile station," *IEEE Tran. Veh. Techol.*, vol. 51, no. 3, pp. 425–434, May 2002.

[6] L. Schumacher, "Recent advances in propagation characterisation and multiple antenna processing in the 3GPP framework," *Proc. of XXVIth URSI General Assembly 2002*, Maastricht, The Netherlands, Aug. 2002.

[7] L. Correia, *Wireless Flexible Personalised Communications - COST 259 Final Report.* John Wiley & Sons, 2001.

[8] P. J. Smith and M. Shafi, "The impact of complexity in MIMO channel models," *ICC'04*, Paris, France, June 2004, pp. 2924–2928.

[9] H. Xu, D. Chizhik, H. Huang, and R. Valenzuela, "A generalized space-time multiple-input multiple-output (MIMO) channel model," *IEEE Trans. Wireless Commun.*, vol. 3, pp. 966–975, May 2004.

[10] 3GPP, TR 25.996, "Spatial channel model for multiple input multiple output (MIMO) simulations (Rel. 6)", 2003.

[11] L. Schumacher, K. I. Pedersen, and P. E. Mogensen, "From antenna spacings to theoretical capacities - guidelines for simulating MIMO systems," *PIMRC 2002*, vol. 2, Sept. 2002, pp. 587–592.

[12] W. C. Y. Lee, "Effects on correlation between two mobile radio base-station antennas," *IEEE Trans. Commun.*, vol.21, pp. 1214–1224, Nov. 1973.

[13] F. Adachi, M. Feeny, A. Williamson, and J. Parsons, "Crosscorrelation between the envelopes of 900MHz signal received at a mobile radio base station site," *Proc. Inst. Elect. Eng.*, vol. 133, Oct. 1986, pp. 506–512.

[14] J. Salz and J. Winters, "Effects of fading correlation on adaptive arrays in digital mobile radio," *IEEE Trans. Veh. Technol.*, vol. 43, pp. 1049–1057, Nov. 1994.

[15] K. I. Pedersen, P. E. Mogensen, and B. H. Fleury, "Spatial channel characteristics in outdoor environments and their impact on BS antenna system performance," *Proc. Veh. Tech. Conf.*, Ottawa, Canada, May1998, pp. 719–724.

[16] J. Salo, G. Del Galdo, J. Salmi, P. Kÿosti, M. Milojevic, D. Laselva, and C. Schneider, (2005, Jan.) "MATLAB implementation of the 3GPP Spatial Channel Model (3GPP TR 25.996)," [Online]. Available: http://www.tkk.fi/Units/Radio/scm.

[17] A. Giorgetti, P. J. Smith, M. Shafi and M. Chiani, "MIMO capacity, level crossing rates and fades: the impact of spatial/temporal channel correlation," *Journal of Communications and Networks,* vol. 5, no. 2, pp 104–115, June 2003.

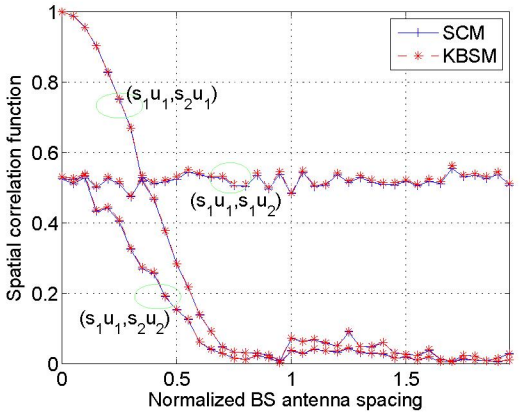

Fig. 6. Spatial correlation functions of the SCM and KBSM averaged at the link level, as functions of the normalized BS antenna spacing ($\Delta d_u/\lambda = 0.2$, $\theta_{BS} = 60$ degree, $\theta_{MS} = 245$ degree, BS AS = 5 degree, MS AS = 35 degree, "Urban microcell" scenario for the SCM, and Gaussian PDFs for both the subpath AoD and AoA offsets for the KBSM).

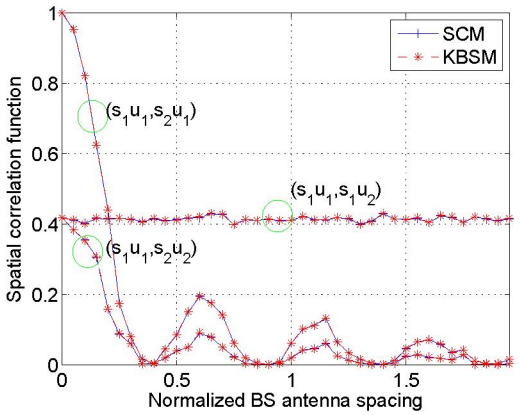

Fig. 7. Spatial correlation functions of the SCM and KBSM averaged at the system level, as functions of the normalized BS antenna spacing ($\Delta d_u/\lambda = 0.2$, BS AS = 5 degree, MS AS = 35 degree, "Urban microcell" scenario for the SCM, and Gaussian PDFs for both the subpath AoD and AoA offsets for the KBSM).